New Mexico Geological Society

Downloaded from: https://nmgs.nmt.edu/publications/guidebooks/76



Interpretation and Results of Large-Scale Aquifer Testing of the San Andres–Glorieta Aquifer in the Sandia Basin, New Mexico

T. Neil Blandford, Farag Botros, Christopher Wolf, and Todd Umstot
2026, pp. 399-408. https://doi.org/10.56577/FFC-76.399

in:

Geology of the Albuquerque Region - Fall Field Conference 2026, Connell, Sean D.; Koning, Daniel J.;, New Mexico Geological Society 76th Annual Fall Field Conference Guidebook, 452 p. https://doi.org/10.56577/FFC-76

This is one of many related papers that were included in the 2026 NMGS Fall Field Conference Guidebook.

Annual NMGS Fall Field Conference Guidebooks

Every fall since 1950, the New Mexico Geological Society (NMGS) has held an annual Fall Field Conference that explores some region of New Mexico (or surrounding states). Always well attended, these conferences provide a guidebook to participants. Besides detailed road logs, the guidebooks contain many well written, edited, and peer-reviewed geoscience papers. These books have set the national standard for geologic guidebooks and are an essential geologic reference for anyone working in or around New Mexico.

Free Downloads

NMGS has decided to make peer-reviewed papers from our Fall Field Conference guidebooks available for free download. This is in keeping with our mission of promoting interest, research, and cooperation regarding geology in New Mexico. However, guidebook sales represent a significant proportion of our operating budget. Therefore, only *research papers* are available for download. *Road logs*, *mini-papers*, and other selected content are available only in print for recent guidebooks.

Copyright Information

Publications of the New Mexico Geological Society, printed and electronic, are protected by the copyright laws of the United States. No material from the NMGS website, or printed and electronic publications, may be reprinted or redistributed without NMGS permission. Contact us for permission to reprint portions of any of our publications.

One printed copy of any materials from the NMGS website or our print and electronic publications may be made for individual use without our permission. Teachers and students may make unlimited copies for educational use. Any other use of these materials requires explicit permission.

This page is intentionally left blank to maintain order of facing pages.

New Mexico Geological Society Guidebook, 76th Fall Field Conference, 2026, p. 399–408, https://doi.org/10.56577/FFC-76.399

INTERPRETATION AND RESULTS OF LARGE-SCALE AQUIFER TESTING OF THE SAN ANDRES–GLORIETA AQUIFER IN THE SANDIA BASIN, NEW MEXICO

T. NEIL BLANDFORD[1], FARAG BOTROS[1], CHRISTOPHER WOLF[1], AND TODD UMSTOT[1]

[1]Daniel B. Stephens & Associates, Inc., 6501 Americas Parkway NE, Suite 200, Albuquerque, NM 87110; nblandford@geo-logic.com

Abstract—This manuscript provides an overview of aquifer testing conducted to quantify well yield and associated drawdown effects for a production well completed in the Permian San Andres–Glorieta aquifer in the Sandia Basin east of the Sandia Mountains in New Mexico. The well is completed in a synclinorium that includes multiple faults and folds. Exploratory boring ASE-1 was drilled to a depth of 3,694 ft (1,126 m) below ground surface (bgs) and was completed with a screen interval from 1,350 to 2,139 ft (411–652 m) bgs in the Permian Abo Formation. This well has a limited yield and may produce up to 50 gallons per minute (gpm) or less. Well ASE-2 was completed nearby in the San Andres and Glorieta Formations with a screen interval from 500 to 690 ft (152–210 m) bgs. The maximum capacity of this well exceeds 1,500 gpm. Aquifer testing of the ASE-2 well was conducted while recording water levels in two San Andres–Glorieta aquifer observation wells and flow at a nearby San Andres–Glorieta aquifer spring. Test results and field observations indicate the presence of high-permeability fracture networks, likely due to solution enhancement of carbonate beds. Although multiple aquifer test solutions and aquifer boundary configurations were considered, we determined that the San Andres–Glorieta aquifer behaves hydrologically as an equivalent porous media, with two low-permeability (i.e., mathematically no-flow) boundaries that coincide with known fault zones and aquifer pinch-outs mapped in the region. We estimate San Andres–Glorieta aquifer hydraulic conductivity within the synclinorium to range from about 450 to nearly 600 feet per day (ft/day).

INTRODUCTION

This manuscript provides an overview of portions of an extensive field investigation and aquifer testing conducted across a large portion of the Sandia Basin. As part of these investigations, we installed and tested two deep wells: ASE-1 and ASE-2 (New Mexico Office of the State Engineer [NMOSE] numbers S-2618-POD1 and S-2618-POD3, respectively). The two wells are 300 ft (91 m) apart. We provide an overview of the geology and hydrogeology of the study area (Fig. 1) based on our investigation and the work of previous authors, and we interpret the results of a long-term aquifer test conducted for ASE-2 in the Permian San Andres–Glorieta aquifer.

GEOLOGIC SETTING

The Sandia Basin has a complex geologic history reflected in the many rock types and geologic structures encountered in the region, ranging in age from Proterozoic to Quaternary (Figs. 2 and 3). The primary geologic units are summarized in Table 1. A geologic cross section (Fig. 2) and block diagram (Fig. 3) illustrate the geologic structure and geometry of the San Andres and Glorieta Formations and other rock units in the study area. The cross section is coincident with the southern edge of the block diagram, which trends east–west through the location of the Wheatfield shallow and deep wells (NMOSE well numbers S-2073 and S-2073-POD2, respectively) south of the ASE wells. Figures 2 and 3 were constructed based on lithological data collected at ASE-1, geologic maps (Read et al., 1995; Ferguson et al., 1999b), and an unpublished surface geophysical survey. Boring ASE-1 penetrated the entire sedimentary stratigraphic sequence from Quaternary alluvium at the land surface to the Pennsylvanian Sandia Formation, with drilling terminated at 3,694 ft (1,126 m) bgs upon encountering intrusive rocks in the Sandia Formation.

Multiple geologic events have fractured, faulted, and folded rocks within the study area (Kelley and Northrop, 1975; Karlstrom et al., 1999; Ferguson et al., 1999b), and many of the rocks at outcrop and encountered during drilling are jointed and fractured. The earliest geologic events date back to the Proterozoic Era, when contractional forces related to early continental development initiated deformation structures observed along the Rio Grande rift (e.g., Karlstrom et al., 1999, 2026). These geologic forces created northeast–southwest structural trends that influenced subsequent geologic structures such as the Tijeras fault zone (Fig. 1).

The next major geologic event was the Ancestral Rocky Mountain orogeny during the Mississippian through Permian Periods. The Pedernal uplift created a mountain range east of the present Sandia Mountains, which supplied much of the sediment that constitutes the Madera, Abo, and Yeso Formations.

The Laramide orogeny occurred in the Late Cretaceous to early Paleogene. This event reactivated many northeast-trending faults with a component of dextral (right-lateral) strike-slip movement, including the Tijeras fault (Fig. 2). Some of the earlier normal faults experienced reverse slip during this period, causing hundreds of feet of offset.

The most recent tectonic event that created the Sandia Mountains is the formation of the Rio Grande rift, which began in the Miocene (Karlstrom et al., 1999). The rift is the result

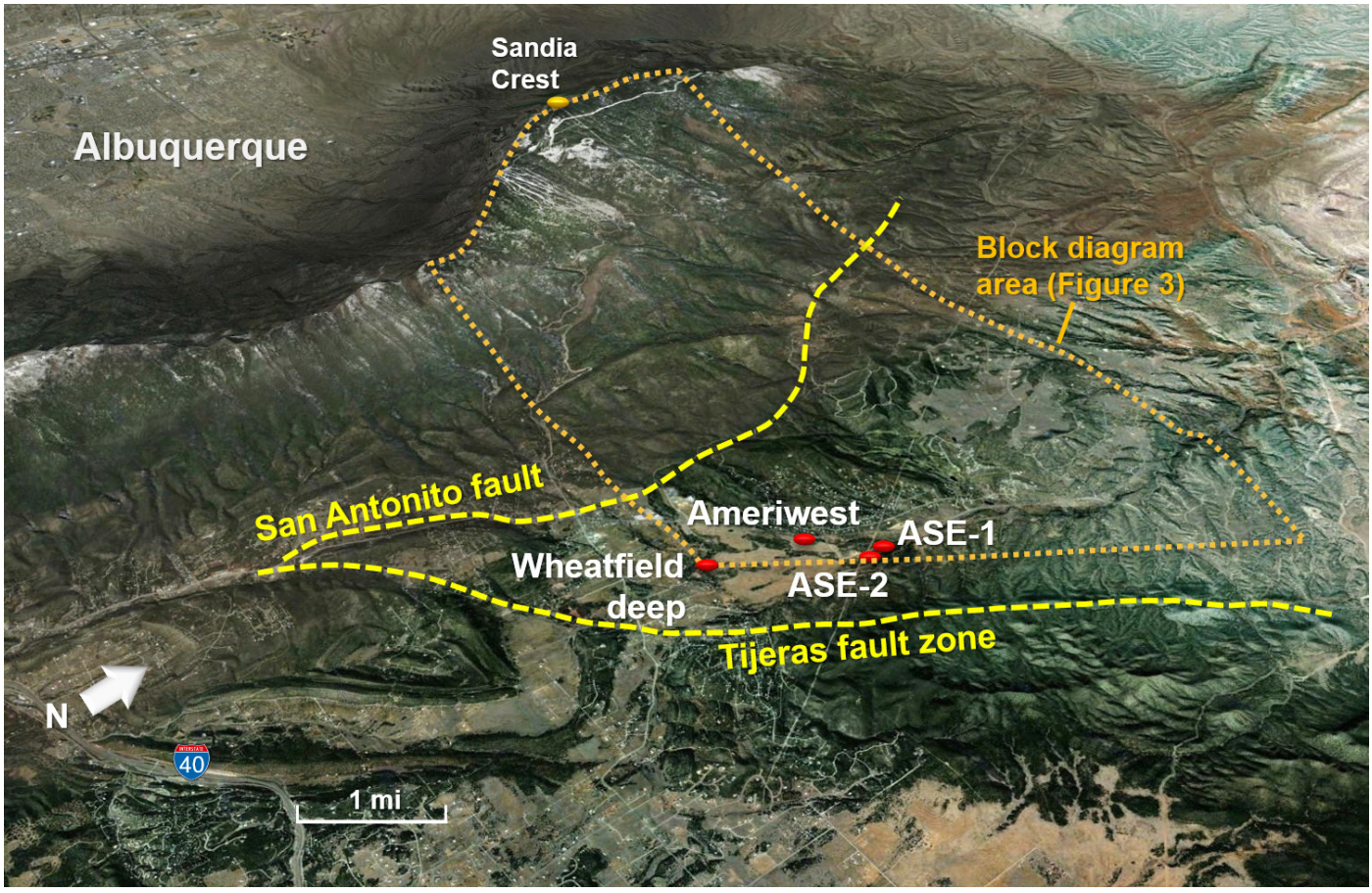


FIGURE 1. Geographic setting of the study area and well locations.

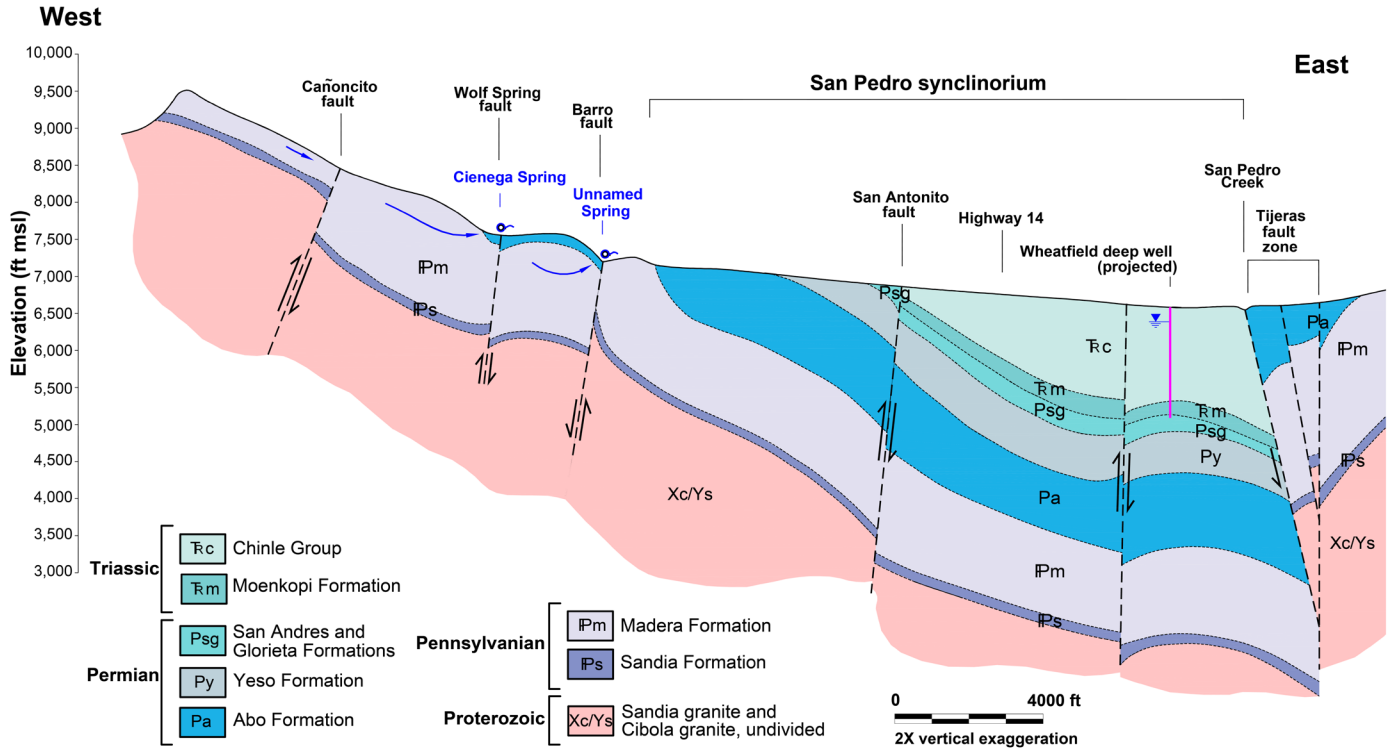


FIGURE 2. Vertically exaggerated west-to-east geologic cross section coincident with the southern edge of the block diagram in Figure 3.

of crustal extension that created a series of north–south-trending basins from Colorado through New Mexico into Texas and northern Mexico (e.g., Hawley, 1996). During the formation of the Rio Grande rift, many right-slip faults were reactivated (e.g., Karlstrom et al., 1999, 2026).

Paleozoic and Mesozoic rocks deposited on Proterozoic crystalline basement dip to the east along the east side of the Sandia Mountains (Fig. 2). Offset of the units is evident along the Cañoncito, Wolf Spring, Barro, and San Antonito faults and the Tijeras fault zone (Figs. 2 and 3). The Tijeras fault zone has a particularly complex geometry, reflecting multiple reactivation events involving normal, reverse, and strike-slip movements over geologic time. This fault zone is considered a Riedel shear zone represented by conjugate faults developed during strike-slip reactivation (Abbott and Goodwin, 1995; Ferguson et al., 1999a). Within the Tijeras fault zone, large fault blocks have been rotated and laterally offset as much as 5,000 ft (1.5 km; Ferguson et al., 1999a).

Wells ASE-1 and ASE-2 are completed in the San Pedro synclinorium (Fig. 2), which consists of several broad, high-amplitude folds that trend northeast and plunge toward the southwest (Kelley and Northrop, 1975; Ferguson et al., 1999b). The Permian San Andres Formation is encountered at about 495 ft (151 m) bgs at the ASE wells and 1,480 ft (451 m) bgs at the Wheatfield deep well (Fig. 3).

HYDROGEOLOGIC FRAMEWORK

The hydrogeology of the study area is controlled by the complex interactions of variable groundwater recharge, geologic structure, and hydraulic properties of the geologic units. Recharge occurs predominantly at higher elevations, with

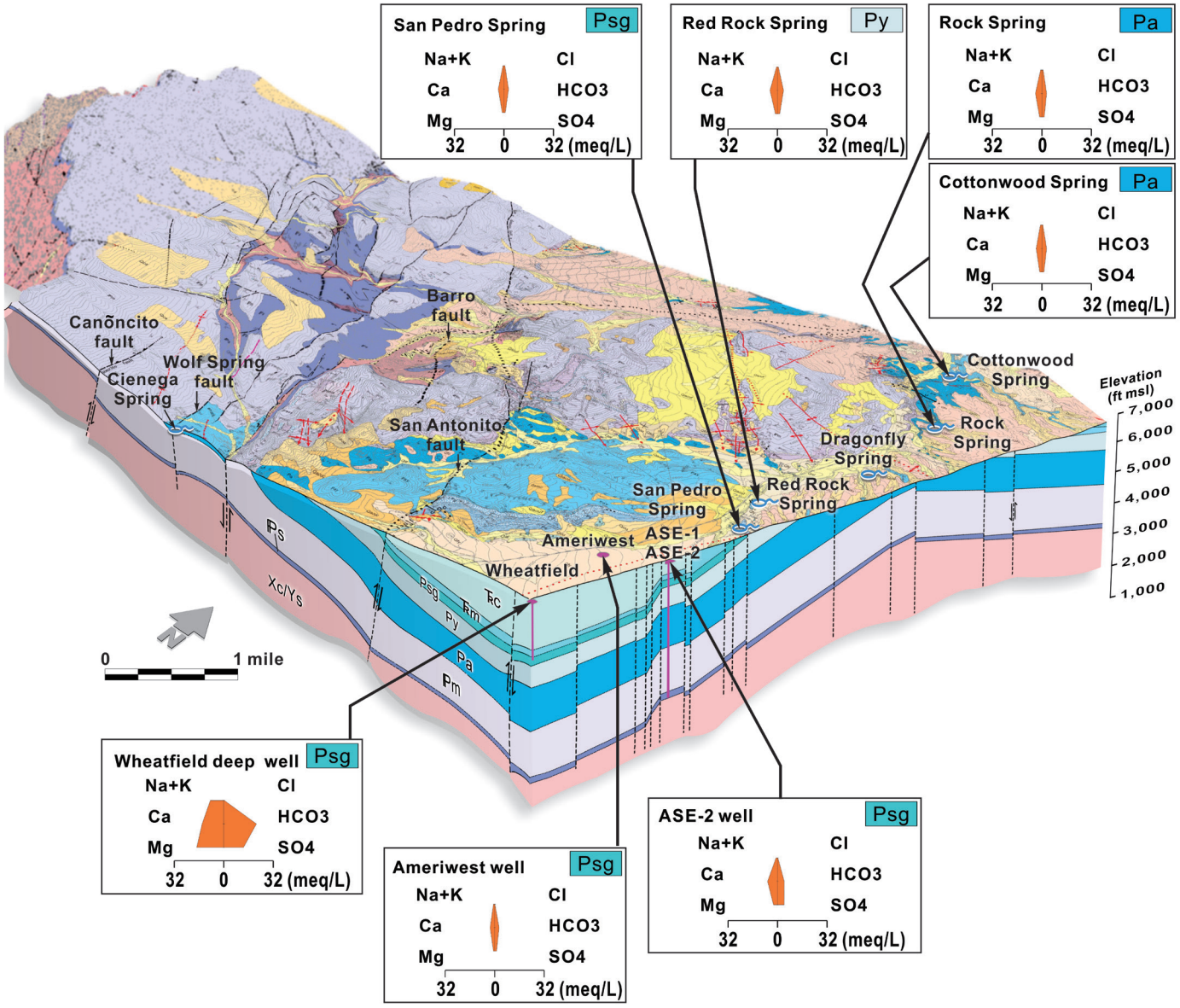


FIGURE 3. Hydrogeologic block diagram showing geologic structures and water quality. The diagram location is shown in Figure 1. At the ASE well locations, only the ASE-1 exploration boring is shown. Well ASE-1 has 789 ft (240 m) of screen in the Abo Formation, and ASE-2 is screened across 190 ft (58 m), which essentially is the full thickness of the San Andres and Glorieta Formations, labeled Psg. The Wheatfield deep well penetrates 40 ft (12 m) into the San Andres–Glorieta aquifer.

infiltration occurring on outcrops and along arroyos. Groundwater generally moves eastward or northward from areas of recharge along the mountain front to areas of discharge, such as wells, springs, or adjacent geologic units (Bartolino et al., 2010).

Predominant study-area aquifers include the Pennsylvanian Sandia and Madera Formations, and the Permian Abo, Yeso, San Andres, and Glorieta Formations (Figs. 2 and 3). Sandstone lenses in the Triassic Chinle Group produce small to moderate amounts of water in the southern portion of the

TABLE 1. Summary of geologic units interpreted in ASE-1.

Period	Unit (Map symbol)	Description	Thickness (ft/m)
Quaternary	Alluvium (Qal)	Red to brown sand and silt with gravel and clay	20/6
Triassic	Chinle Group (Trc)	Dark red shale and feldspathic sandstone	340/104
	Moenkopi Fm (Trm)	Dark red, micaceous siltstone and sandstone	135/41
Permian	San Andres Fm (Ps)	Gray, medium- to thick-bedded limestone with quartz sand	205/62 (Ps + Pg)
	Glorieta Fm (Pg)	White to pink, well-sorted, quartz arenite	
	Yeso Fm (Py)	Orange-red sandstone and siltstone with occasional limestone.	540/165
	Abo Fm (Pa)	Dark-red nonmarine sequence of generally fine-grained arkosic conglomerate, sandstone, siltstone, and shale with thin beds of limestone.	1,040/317
Pennsylvanian	Madera Fm (IPm)	Wild Cow member contains arkosic sandstone, sandstone, conglomerate, siltstone, shale, and calcarenite.	785/239
		Gray limestone, sandstone, and conglomerate.	500/152
	Sandia Fm (IPs)	Olive green siltstone, sandstone, and conglomerate	129/39
Proterozoic	Sandia and Cibola granite, undivided (Xc/Ys)	Granite and monzogranite with potassium feldspar and biotite	Basement

Note: Combined San Andres (Ps) and Glorieta (Pg) Formations are denoted as Psg on figures.

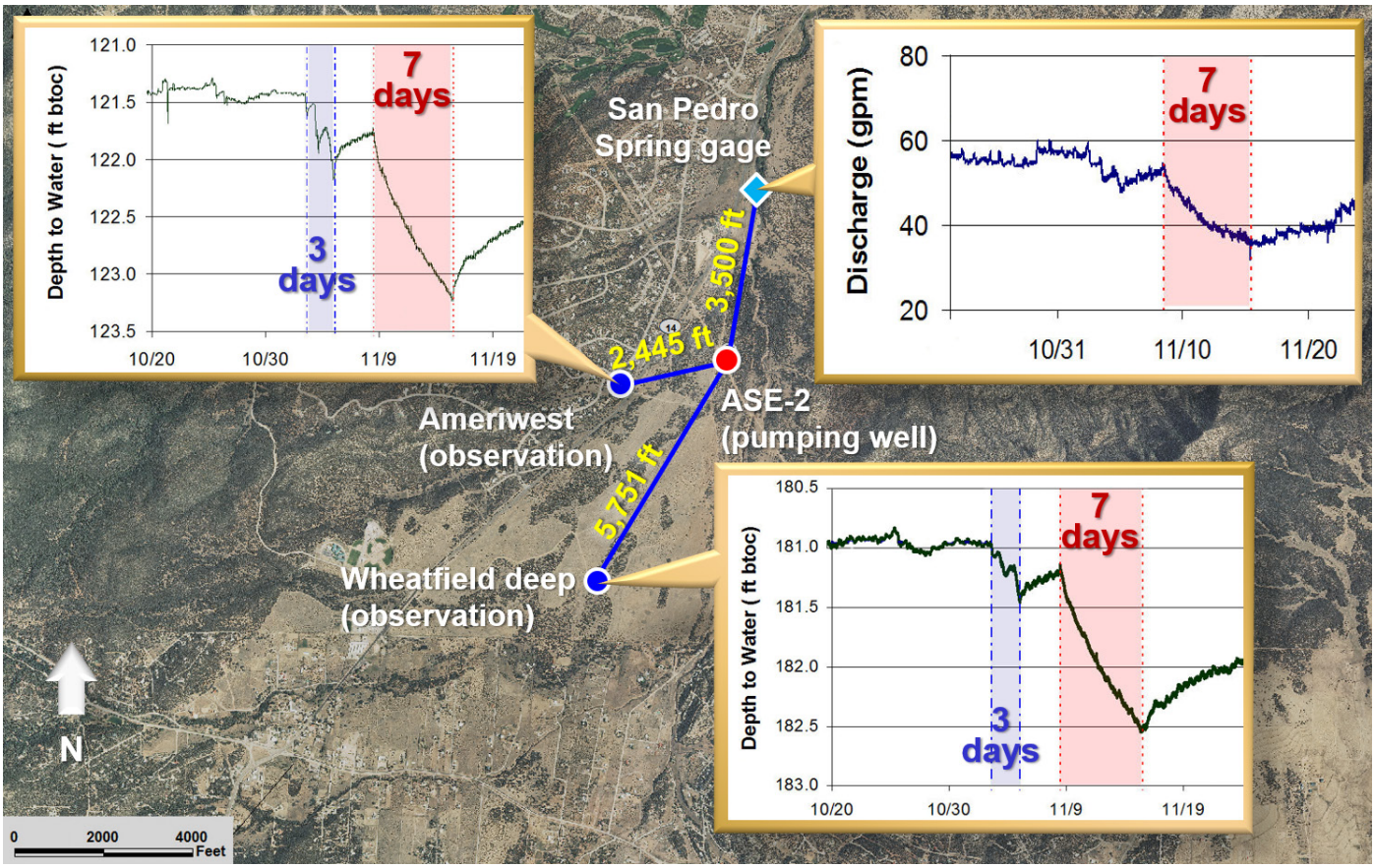


FIGURE 4. Well ASE-2 aquifer test configuration, observed San Andres–Glorieta aquifer water levels, and San Pedro spring flow.

study area. We initially targeted the Madera Formation, which yielded little to no water at ASE-1. The Abo and Yeso Formations typically yield sufficient water for domestic wells, but not in large volumes. Well ASE-1 is completed in the Abo Formation (1,350–2,139 ft [411–652 m] bgs) and has a small yield. The San Andres and Glorieta Formations can each yield significant quantities of water to wells (Shafike and Flanigan, 1999). Combined, these two formations comprise the San Andres–Glorieta aquifer, the most productive aquifer in the study area. Well ASE-2 is completed in the San Andres–Glorieta aquifer and is screened from 500 to 690 ft (152–210 m) bgs.

The relationships between rock units and structures, and their influence on groundwater flow and chemistry, are illustrated in a block diagram (Fig. 3). Springs tend to occur where geologic structures truncate aquifer units at the surface (Ferguson et al., 1999a). Rock types and seepage between aquifer units influence water quality, as shown by the stiff diagrams in Figure 3. For example, ASE-2 is completed through the full thickness of the San Andres–Glorieta aquifer, and water from this well includes upward seepage of water from the underlying Yeso Formation, which has a high gypsum content. The nearby Ameriwest well (NMOSE well number S-1065 Expl-1) is also completed in the San Andres–Glorieta aquifer but does not penetrate the full thickness of the Glorieta Formation. Water from this well has lower sulfate and total dissolved solids concentrations compared to water from ASE-2. The Ameriwest well has similar water quality to that observed at San Pedro spring. Groundwater generally flows northward (i.e., from the ASE-2 and Ameriwest wells toward San Pedro spring) in the updip direction.

San Pedro Creek (Fig. 3) is the primary surface-water feature in the study area. Perennial flow in the creek is limited to reaches downstream of springs that occur along the creek. San Pedro spring, the largest spring in the study area, discharges at about 60 gpm and forms the first and longest perennial reach (~2 mi [~3.2 km]) of San Pedro Creek. The spring occurs where rocks of the San Andres–Glorieta aquifer crop out in the creek bed, generally covered by a thin veneer of alluvium, at the north end of the San Pedro synclinorium (Fig. 3).

METHODS

Step-test and constant-rate aquifer tests were conducted on ASE-1 and ASE-2. Step tests were used to calculate well efficiency and to determine the pumping rate for the constant rate tests. For each aquifer test, the pumping well was equipped with a pressure transducer set in a 2-inch (5-cm)-diameter sounding tube to measure water levels during the pumping and recovery phases of the test. Water levels were also manually gauged to confirm the transducer measurements. Pumping rates were measured using a digital flow meter and a backup meter.

Throughout the pumping and recovery periods, water levels were monitored using pressure transducers and manual methods in the Wheatfield shallow, Wheatfield deep, and Ameriwest wells (Figs. 1 and 4). The Ameriwest and Wheatfield deep wells are completed in the San Andres Formation, while the Wheatfield shallow well is completed in the Triassic Chinle Group. Only the Wheatfield deep well (not the Wheatfield shallow well) is shown in the figures. San Pedro spring discharge was monitored throughout drilling and testing activities using a temporary weir constructed across the stream channel. The distances between ASE-2 and the San Andres–Glorieta aquifer observation points are provided in Figure 4.

Well ASE-2 discharge water was piped south from the test wells to a network of temporary sprinkler systems operated during the test. As the San Andres–Glorieta aquifer is present at about 500 ft (152 m) bgs, beneath low-permeability Chinle Group sediments, water discharged at the surface could not affect the observed water levels during the pumping or recovery periods. Aquifer test discharge was not released to San Pedro Creek so that spring discharge could be monitored during the test without undue interference.

AQUIFER TEST RESULTS

The results of the step-drawdown tests at ASE-1 and ASE-2 are provided in Table 2. Well ASE-1 has very limited production potential, and only two pumping steps were conducted. The specific capacity of this well is about 0.1 gpm per foot of drawdown (gpm/ft). The step-drawdown test conducted on well ASE-2 indicated that the well is highly productive, exhibiting a specific capacity of about 30 to 40 gpm/ft for lower pumping rates and about 17 gpm/ft for the highest tested rate of 1,600 gpm (Table 2).

The ASE-1 constant rate test was a single-well test (there were no Abo Formation observation wells) that confirmed the limited production capacity of the Abo Formation. Well ASE-1 was pumped at 50 gpm for 4.25 days and experienced about 926 ft (282 m) of drawdown. Analysis of the test results indicated an average hydraulic conductivity of 0.005 to 0.03 ft/day for the screened interval.

The ASE-2 constant-rate aquifer test was conducted in November 2010 for 7 days at a pumping rate of 850 gpm. The step testing indicated that ASE-2 can pump nearly twice this rate, but the test rate was selected to significantly perturb the

TABLE 2. Summary of well ASE-1 and ASE-2 step-drawdown tests.

Well Step	Step Duration (min)	Discharge Rate (gpm)	Drawdown (ft)	Specific Capacity (gpm/ft)
ASE-1				
1	120	50	493.5	0.1
2	60	60	796.4	0.1
ASE-2				
1	200	400	9.5	42
2	200	700	23.5	30
3	200	1,000	41.7	24
4	200	1,300	68.5	19
5	200	1,600	96.8	17

Note: gpm = gallons per minute; gpm/ft = gallons per minute per foot of drawdown.

aquifer system while maintaining a manageable quantity of discharge. Total drawdown at ASE-2 after 7 days of pumping was about 31 ft (~9 m).

Figure 4 illustrates the observed hydraulic head and spring discharge response during the ASE-2 aquifer test. Nearly immediate responses to pumping at ASE-2 were observed in the Ameriwest and Wheatfield deep wells and at the San Pedro spring gauge, followed by nearly immediate recovery trends at the cessation of pumping. Total uncorrected drawdown at the end of the test was 1.6 ft (0.5 m) at the Ameriwest well and 1.4 ft (0.4 m) at the Wheatfield deep well, even though the Wheatfield deep well is more than twice the distance from ASE-2 than the Ameriwest well (Fig. 4). The Wheatfield deep well is downdip within the synclinorium, where the top of the San Andres–Glorieta aquifer is about 707 ft (215 m) deeper than the bottom of the screen in well ASE-2, and San Pedro spring is updip, about 405 ft (123 m) higher in elevation than the top of the screen in well ASE-2. Flow at San Pedro spring, about 3,500 ft (~1 km) north of ASE-2, declined by about 14 gpm by the end of the test (Fig. 4).

Drawdown from ASE-2 well development and step testing are also evident at the Ameriwest and Wheatfield deep observation wells, as highlighted in Figure 4 for the 3-day period prior to the 7-day constant rate test. No drawdown from ASE-2 pumping was observed at the ASE-1 Abo Formation well or at the Wheatfield shallow Chinle Group well.

Barometric pressure was monitored during the tests, but the effects of barometric pressure changes on drawdown were small relative to the observed drawdown; the observed drawdown was not adjusted for these changes.

AQUIFER TEST ANALYSIS AND INTERPRETATION

For our analysis, we assumed that the pumping and observation wells fully penetrate the San Andres–Glorieta aquifer, which is 200 ft (61 m) in thickness. This condition is confirmed for the pumping well, but the Ameriwest and Wheatfield deep wells penetrate only the upper portion of the aquifer, consisting of the San Andres Formation limestone, with some interbedded sandstone of the Glorieta Formation. As both formations are productive and contain no significant low-permeability units, our assumption that the hydraulic head is virtually the same within each formation is reasonable.

In addition, we focused on the simulation of observed drawdown at the Ameriwest and Wheatfield deep wells, which is not influenced by well efficiency. Because the ASE-2 aquifer test was initiated prior to full recovery of the water levels in the Ameriwest and Wheatfield deep monitor wells to static conditions after the step test, the observed drawdown at these wells was adjusted to account for the residual recovery trend. The correction is illustrated in Figure 5 for the Wheatfield deep well.

We also adjusted the observed drawdown in ASE-2 to account for well efficiency, which was determined to be 32% at a pumping rate of 850 gpm using the method of Bierschenk (1963) applied to the step-test data. This low calculated efficiency may be attributable to turbulent flow near the well. We qualitatively considered the adjusted drawdown curve for ASE-2 during our analysis of the test results, but did not include it in our goodness-of-fit calculations.

We applied the aquifer test analysis software AQTESOLV (Duffield, 2007) and custom programming to examine whether alternative aquifer test solutions could reasonably simulate the observed drawdown and recovery data at each observation well. AQTESOLV allows simultaneous fitting of both drawdown and recovery data across multiple wells. Initial simulations indicated that aquifer test solutions, such as Theis (1935), which assumes infinite aquifer extent, could replicate the observed drawdown at each observation well individually; however, they could not produce a solution that fit the observed data at both observation wells simultaneously. To identify a solution that simultaneously fits the drawdown and recovery data from the two monitor wells, we evaluated multiple aquifer test solutions, aquifer boundary configurations, and anisotropic aquifer conditions based on the hydrogeologic setting of the study area. For example, we applied the Moench (1984) solution to analyze aquifer test results for dual-porosity media as one alternative. We identified two aquifer test solutions that provide a good simultaneous match to the observed data, as explained below.

Parallel No-Flow Boundary Aquifer Model

The first aquifer test solution we identified that produced a good match to the observed data was the Theis (1935) solution with two parallel no-flow boundaries. Parallel no-flow boundaries were applied due to limitations in the analytical solution approach for incorporating boundary conditions. One boundary was approximately coincident with the Tijeras fault zone. The second boundary was placed parallel to the first boundary at a distance of 2.3 mi (3.7 km). The distance between the boundaries is the approximate distance between the Tijeras fault zone and the San Antonito fault in the vicinity of the Wheatfield deep well (Fig. 6). Alternative distances between the two boundaries were considered in sensitivity analysis, but the 2.3 mi (3.7 km) distance led to the best fit between the simulated and observed drawdown data. Distances of less than about 1.9 mi (~3.1 km) led to significant degradation of the root-sum-of-squares (RSS) differences between the simulated and observed drawdown at the two observation wells.

The San Antonito fault trends northeast in the southern part of the study area, but it strikes predominantly north within the study area and eventually northwest (Fig. 6). In addition, in the northern portion of the study area, the San Andres–Glorieta aquifer pinches out between the San Antonito fault and ASE-2. For these reasons, the assumed western no-flow boundary in the analytical solution is highly approximate. These limitations on the western no-flow boundary configuration are better addressed in the wedge aquifer solution discussed below, and have been addressed in numerical modeling not presented here.

The results of the parallel no-flow boundary analysis are presented in Figure 7. This analysis yielded San Andres–Glorieta aquifer hydraulic conductivity and storage coefficient values of 452 ft/day and 1.5×10^{-3}, respectively.

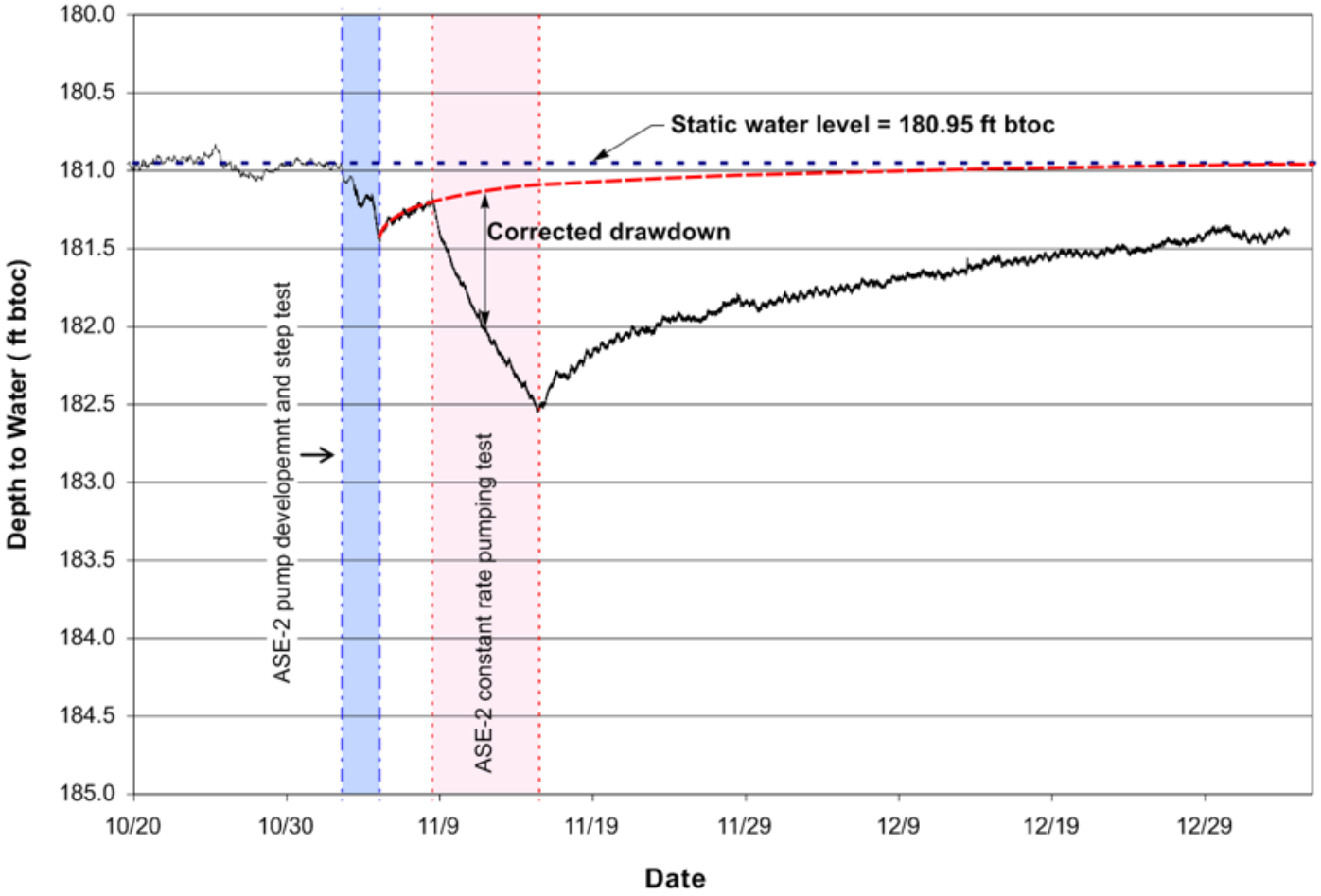


FIGURE 5. Observed and corrected drawdown at the Wheatfield deep well. Drawdown was adjusted to account for the projected residual increase in water levels (dashed red line) after completion of the ASE-2 step test.

We also considered that horizontal anisotropy in aquifer hydraulic conductivity might be an alternative or supplemental explanation for the observed drawdown response at the Ameriwest and Wheatfield deep wells. We tested the cases of no aquifer boundaries, one aquifer boundary coincident with the Tijeras fault zone, and two parallel aquifer boundaries as described above. Horizontal anisotropy was simulated in the aquifer test solutions using a coordinate-transformation approach described in Freeze and Cherry (1979). Hydraulic conductivity in the direction of the San Pedro synclinorium strike (approximately the same alignment as between the ASE-2 and Wheatfield deep wells, parallel to the Tijeras fault zone) was considered to be K_1, and hydraulic conductivity in the transverse direction was considered to be K_2. If horizontal anisotropy is an explanation for the aquifer test results, where the observed drawdown in the observation wells is similar in magnitude, but the Wheatfield deep well is over twice the distance from ASE-2 than the Ameriwest well (Fig. 4), the magnitude of K_1 would be greater than K_2. The coordinate transformation is made by adjusting the real-world coordinates in the transverse direction by the factor $\sqrt{K_1}/\sqrt{K_2}$.

Our analysis indicated that the best fit between the simulated and observed drawdown at the two observation wells is provided by the isotropic hydraulic conductivity case with two parallel no-flow boundaries. However, cases where K_1 was greater than K_2 by a factor of 4 or less yielded a similar RSS value, but slightly worse. When the anisotropy factor was increased from 4 to 9, the RSS was significantly worse.

Wedge Boundary Aquifer Model

We developed a second aquifer test solution for the case of two barrier boundaries that intersect at an angle (Ferris et al., 1962), herein called the wedge aquifer solution. We think this solution better represents the geometry of the interpreted no-flow boundary features than the parallel no-flow boundary solution. We selected an angle of 20° between two converging no-flow boundaries that intersect in the approximate region where the Tijeras fault zone and the San Antonito fault meet (Fig. 8). The eastern boundary of the wedge is approximately coincident with the Tijeras fault zone, and the western boundary of the wedge is approximately coincident with the San Antonito fault in the southern portion of the wedge and strikes between the San Antonito fault and the outcrop of the San Andres and Glorieta Formations in the northern portion of the wedge (Fig. 8). The results of the wedge aquifer analysis are presented in Figure 9. This analysis yielded San Andres–Glorieta aquifer

hydraulic conductivity and storage coefficient values of 590 ft/day and 2.1 x 10^{-3}, respectively.

Interpretation of Aquifer Boundaries

Fault zones in the Sandia Basin have been recognized by previous authors as barriers or impediments to groundwater flow. The Tijeras fault zone was identified as a hydrologic barrier by Titus (1980), Kues (1990), and McCoy and Blanchard (2008). Bartolino et al. (2010) also identified the Tijeras fault zone as a low-permeability feature based on water-level and water-quality data. Although Ferguson et al. (1999a) stated that rocks within about 300 ft (91 m) "of the fault are highly fractured and cut by a myriad of high-angle faults," they also described the fault zone as a "tectonic melange" with blocks of rock that have been translated into position and "rotated significantly" due to movement along the fault. Fractures, where open, would occur within rotated and displaced blocks that disrupt fracture continuity. In addition, we observed in the field fractures and bedding planes in the fault zone that contained variable amounts of fault gouge or diagenetic minerals (e.g., carbonates), which would also decrease fracture permeability.

To our knowledge, the San Antonito fault has not been previously identified as a barrier to groundwater flow. The San Antonito fault is not as extensive as the Tijeras fault zone, but it consists of multiple faults and has experienced strike-slip movement, in addition to variable amounts of vertical offset along its mapped length (Ferguson et al., 1999a; Ferguson et al., 1999b). In the southern portion of the study area, such as the area west of the Wheatfield deep well, we interpret that offset along the fault and possibly other conditions, such as fault gouge, essentially form a no-flow aquifer boundary. In the northern portion of the San Pedro synclinorium, the San Antonito fault does not affect groundwater flow in the San Andres–Glorieta aquifer because the San Andres and Glorieta Formations crop out and are truncated between the fault and the Ameriwest well (Fig. 8). In this northern region of the synclinorium, the no-flow boundary condition is attributable to pinch-out of the aquifer rather than offset of geologic units at the fault.

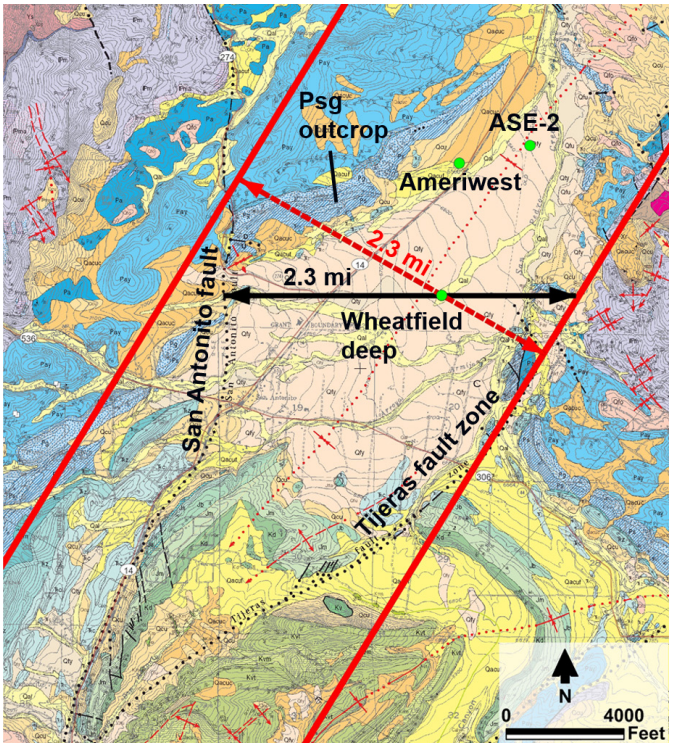


FIGURE 6. No-flow boundary orientation (red lines) for parallel boundary analytical solution (Theis, 1935). Geologic base map from Ferguson et al. (1999b).

Production Capacity of the San Andres–Glorieta Aquifer

The nearly immediate hydraulic response to pumping over a significant portion of the aquifer could be due to a karstic aquifer system within limestone of the San Andres Formation. Although it is likely that solution channels and conduits exist in the San Andres Formation, the sandstone of the Glorieta Formation was observed to be fractured in drill cuttings. A temporary test well was installed during the drilling of ASE-1 to evaluate water quality and estimate pumping capacity within the midsection of the fractured sandstone of the Glorieta Formation. The temporary well had 20 ft (6 m) of screen at 655 ft (200 m) bgs and 60 ft (18 m) of gravel pack at 645 ft (197 m) bgs. This zone was isolated using a bentonite seal and pumped for more than 500 minutes at 90 and 140 gpm, and the observed drawdown indicated a specific capacity of about 10 to 15 gpm/ft. Compared to the ASE-2 specific capacity of 27 gpm/ft determined from the aquifer test, and considering that ASE-2 is screened across the full San Andres and Glorieta Formation thickness, we infer that the fractured sandstone

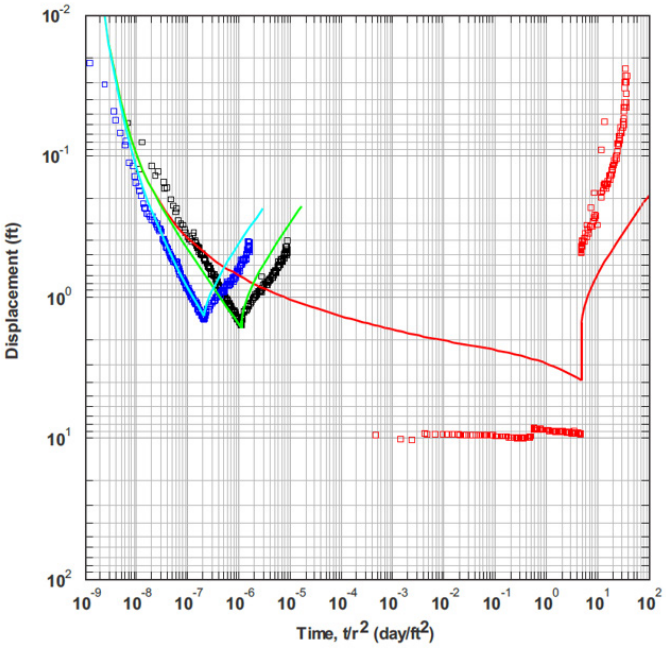


FIGURE 7. Simulated curve fit (solid line) and observed data points (squares) for parallel no-flow boundary solution. Blue is the Wheatfield deep observation well, green is the Ameriwest observation well, and red is the ASE-2 pumping well. The curve fit at ASE-2 was qualitatively considered.

of the Glorieta Formation contributes approximately half of the ASE-2 well yield and possibly more, as the diameter and screen length of the temporary test well at ASE-1 were limited.

DISCUSSION AND CONCLUSIONS

The ASE-2 aquifer test results indicate a highly permeable aquifer with efficient hydraulic connection through fracture networks, likely enhanced by solution activity within carbonate strata. Drawdown at the Ameriwest and Wheatfield deep wells and reduction in flow at San Pedro spring were nearly instantaneous with the onset of pumping. This result was not necessarily expected, particularly for the Wheatfield deep well, where lower permeability was anticipated due to the greater formation depth and lower expected solution enhancement of permeability, as the aquifer is more isolated from near-surface recharge sources.

Our analysis of the test results shows that two aquifer no-flow boundaries are recognized in the observed water-level responses at the Ameriwest and Wheatfield deep wells. The eastern no-flow boundary corresponds to the Tijeras fault zone. We interpret the other boundary to be a combination of the San Antonito fault in the southern portion of the synclinorium and the pinch-out of the San Andres–Glorieta aquifer in the northern portion of the synclinorium. Anisotropy in horizontal hydraulic conductivity could not be ruled out based on the observed data.

Although the San Andres–Glorieta aquifer is known to pinch out north of ASE-2 in the vicinity of San Pedro spring, consideration of this region as a no-flow boundary perpendicular to the Tijeras fault zone did not significantly improve the aquifer parameter estimation results. One reason the effects of the northern pinch-out may be limited is that the reduction in spring flow is a source of water to ASE-2. To some extent, these two boundary conditions (i.e., hydrologic barrier, and source of water to the well) will offset one another.

Constant-rate aquifer tests are typically conducted for 24 or 72 hours, at pumping rates similar to or sometimes less than the expected long-term rate. If the ASE-2 aquifer test had been conducted for 24 hours, only one no-flow boundary would have been recognized from the observed drawdown response, and a 72-hour test would have been sufficient to detect the second aquifer boundary. If the rate had been equal to the planned operational pumping rate for the well rather than nearly double the planned rate, a 72-hour aquifer test would have been insufficient to conclusively detect the second no-flow aquifer boundary.

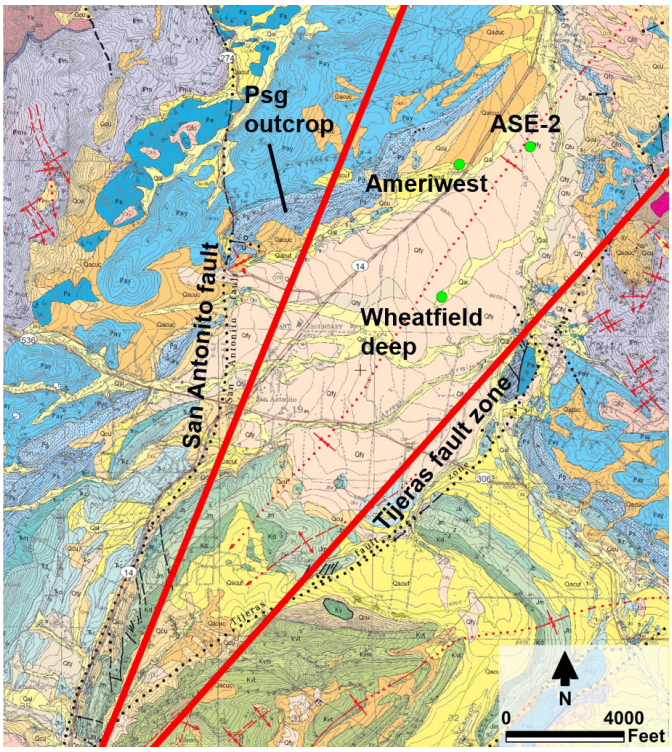


FIGURE 8. No-flow boundary orientation (red line) for wedge aquifer analytical solution (Theis, 1935). Geologic base map from Ferguson et al. (1999b).

ACKNOWLEDGMENTS

We thank Andre Ritchie and Dr. John Shomaker for their thorough reviews, helpful comments, and suggestions.

REFERENCES

Abbott, J.C., and Goodwin, L.B., 1995, A spectacular exposure of the Tijeras fault, with evidence for Quaternary motion: New Mexico Geological Society, Guidebook 46, p. 117–125. https://doi.org/10.56577/FFC-46.117

Bartolino, J.R., Anderholm, S.K., and Myers, N.C., 2010, Groundwater resources of the East Mountain area, Bernalillo, Sandoval, Santa Fe, and Torrance Counties, New Mexico, 2005: U.S. Geological Survey Scientific Investigations Report 2009–5204, 81 p. https://doi.org/10.3133/sir20095204

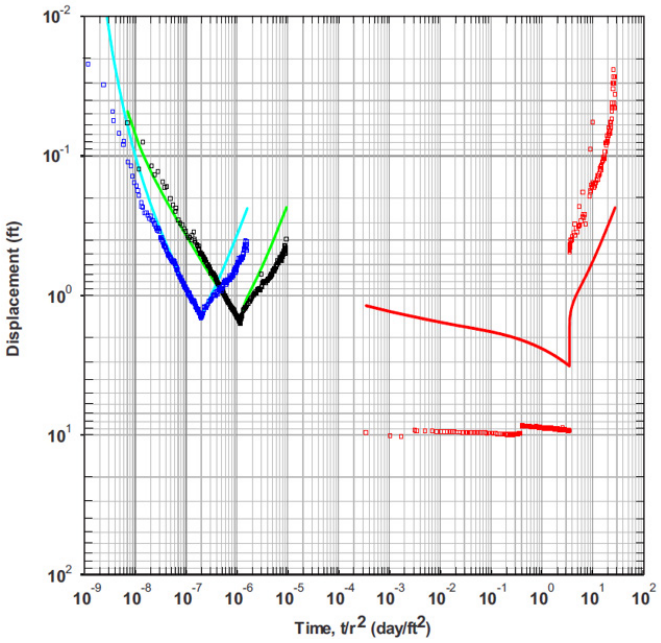


FIGURE 9. Simulated curve fit (solid line) and observed data points (squares) for wedge aquifer analytical solution. Blue is the Wheatfield deep observation well, green is the Ameriwest observation well, and red is the ASE-2 pumping well. The curve fit at ASE-2 was qualitatively considered.

Bierschenk, W.H., 1963, Determining well efficiency by multiple step-drawdown tests: International Association of Science, Hydrology, v. 64, p. 493–507.

Duffield, G.M., 2007, AQTESOLV for Windows, Version 4.50.002, Professional. Developed by HydroSOLVE, Inc. for ARCADIS Geraghty & Miller, Inc.

Ferguson, C.A., Timmons, J.M., Pazzaglia, F.J., Karlstrom, K.E., Osburn, G.R., and Bauer, P.W., 1999a, Geology of Sandia Park quadrangle, Bernalillo and Sandoval Counties, New Mexico: New Mexico Bureau of Mines and Mineral Resources Open-file Geologic Map 1, scale 1:24,000. https://doi.org/10.58799/OF-GM-1

Ferguson, F.A., Osburn, G.R., and Allen, B.D., 1999b, Geologic map of the San Pedro 7.5 - minute quadrangle: New Mexico Bureau of Geology and Mineral Resources, Open-file Geologic Map 29, scale 1:24,000. https://doi.org/10.58799/OF-GM-29

Ferris, J.G., Knowles, D.B., Brown, R.H., and Stallman, R.W., 1962, Theory of aquifer tests: U.S. Geological Survey Water-Supply Paper 1536 E, 174 p. https://pubs.usgs.gov/wsp/wsp1536-E/

Freeze, R.A., and Cherry, J.A., 1979, Groundwater: Englewood Cliffs, New Jersey, Prentice-Hall Inc., 604 p.

Hawley, J.W., 1996, Hydrogeologic framework of potential recharge areas in the Albuquerque Basin, central Valencia County, New Mexico, *in* Hawley, J.W. and Whitworth, T.M., eds., Hydrogeology of Potential Recharge Areas for the Basin- and Valley-Fill Aquifer Systems, and Hydrogeochemical Modelling of Proposed Artificial Recharge of the Upper Santa Fe Aquifer, northern Albuquerque Basin, New Mexico: New Mexico Bureau of Mines and Mineral Resources, Open-file Report 402-D, p. 1–68. https://doi.org/10.58799/OFR-402D

Karlstrom, K.E., Cather, S.M., Kelley, S.A., Heizler, M.T., Pazzaglia, F.J., and Roy, M., 1999, Sandia Mountains and Rio Grande rift: Ancestry of structures and history of deformation: New Mexico Geological Society, Guidebook 50, p. 155–165. https://doi.org/10.56577/FFC-50.155

Karlstrom, K.E., Ricketts, J.W., Thacker, J.O., Heizler, M.T., Lucas, S.G., Crossey, L.J., and Connell, S.D., 2026, Tectonics of the Sandia Mountains: 50 years after Kelley and Northrop's memoir: New Mexico Geological Society, Guidebook 76, this volume

Kelley, V.C., and Northrop, S.A., 1975, Geology of Sandia Mountains and vicinity, New Mexico: New Mexico Bureau of Mines and Mineral Resources, Memoir 29, 136 p. https://doi.org/10.58799/M-29

Kues, G., 1990, Ground-water availability and quality in eastern Bernalillo County and vicinity, central New Mexico: U.S. Geological Survey Water-Resources Investigations Report 89-4127, 82 p. https://doi.org/10.3133/wri894127

McCoy, K.J., and Blanchard, P.J., 2008, Precipitation, ground-water hydrology, and recharge along the eastern slopes of the Sandia Mountains, Bernalillo County, New Mexico: U.S. Geological Survey Scientific Investigations Report 2008–5179, 34 p. https://doi.org/10.3133/sir20085179

Moench, A.F., 1984, Double-porosity models for a fissured groundwater reservoir with fracture skin: Water Resources Research, v. 20, no. 7, p. 831–846. https://doi.org/10.1029/WR020i007p00831

Read, A.S., Karlstrom, K.E., Connell, S., Kirby, E., Ferguson, C.A., Ilg, B., Osburn, G.R., Van Hart, D., and Pazzaglia, F.J., 1995, Geology of Sandia Crest quadrangle, Bernalillo and Sandoval Counties, New Mexico: New Mexico Bureau of Geology and Mineral Resources Open-file Geologic Map 6, scale 1:24,000. https://doi.org/10.58799/OF-GM-6

Shafike, N.G., and Flanigan, K.G., 1999, Hydrologic modeling of the Estancia Basin, New Mexico: New Mexico Geological Society, Guidebook 50, p. 409–418. https://doi.org/10.56577/FFC-50.409

Theis, C.V., 1935, The relation between the lowering of the piezometric surface and the rate and duration of discharge of a well using groundwater storage: EOS, Transactions of the American Geophysical Union, v. 16, no. 2, p. 519–524. https://doi.org/10.1029/TR016i002p00519

Titus, F.B., Jr., 1980, Ground water in the Sandia and northern Manzano Mountains, New Mexico: New Mexico Bureau of Mines and Mineral Resources, Hydrologic Report 5, 66 p. https://doi.org/10.58799/HR-5